JOURNAL OF CATALYSIS 92, 1–10 (1985)

Laser Raman Characterization of Tungsten Oxide Supported on Alumina: Influence of Calcination Temperatures

SHIRLEY S. CHAN,[1] ISRAEL E. WACHS, LAWRENCE L. MURRELL, AND NICK C. DISPENZIERE, JR.

Corporate Research–Science Laboratories, Exxon Research and Engineering Company, Annandale, New Jersey 08801

Received March 12, 1984; accepted October 25, 1984

The influence of calcination temperature upon the solid state chemistry of WO_3 on Al_2O_3 was examined with laser Raman spectroscopy. Laser Raman spectroscopy revealed the amorphous and crystalline structural transformations occurring in the WO_3 on Al_2O_3 oxide system. Below monolayer coverage of tungsten oxide on alumina, the tungsten oxide phase is present as a highly dispersed and amorphous surface complex on the support. A close-packed monolayer of the tungsten oxide surface complex on alumina is formed as the surface area of the alumina support decreases at high calcination temperatures. The lower the tungsten oxide loading, the more severe the calcination temperature must be to reach the close-packed monolayer. The close-packed tungsten oxide monolayer accommodates the further desurfacing at still higher temperatures by forming the bulk tungsten oxide phases WO_3 and $Al_2(WO_4)_3$. The $Al_2(WO_4)_3$ phase is formed from the reaction of WO_3 crystallites with the Al_2O_3 support. The parameter controlling the phases present in the WO_3 on Al_2O_3 system is the *surface density* of the tungsten oxide species on the alumina surface.

I. INTRODUCTION

The alumina-supported tungsten oxide system, WO_3 on Al_2O_3, has been examined with many different characterization techniques in recent years: temperature programmed reduction (TPR) (*1*), laser Raman spectroscopy (LRS) (*1–5*), and X-ray photoelectron spectroscopy (XPS) (*5, 6*), uv-visible diffuse reflectance spectroscopy (*3, 4*), and X-ray diffraction (XRD) (*3, 4*). Some controversy exists in the literature as to whether tungsten oxide is octahedrally or tetrahedrally coordinated to the alumina surface (*1–5*). The studies to date have primarily concentrated on the state of tungsten oxide on the alumina surface as a function of tungsten loading at calcination temperatures of 500–550°C. Increasing the tungsten oxide concentration to monolayer coverage on the alumina surface shifts the major Raman peak associated with the tungsten oxide surface species from ~965 to ~1000 cm^{-1} (*1–4*), and shifts the TPR peak to lower temperatures (*1, 2*). These changes have been attributed to either the heterogeneous nature of the alumina surface and/or lateral interactions between tungsten oxide surface species with increasing coverage (*1–4*). Recent *in situ* studies have revealed that the shifts in the Raman bands are associated with the coordination of water molecules with the surface oxide species, and that lateral interactions can, either sterically or electronically, influence the number of water molecules that may be coordinated to the surface oxide species (*7, 8*). Furthermore, the extent of hydration of the surface oxide species is at a minimum at monolayer coverage due to steric interactions where lateral interactions are at a maximum. Above one monolayer coverage of tungsten oxide on alumina, crystallites of WO_3 are formed which can be detected by LRS (*1–5*). One study has also briefly examined the influence of

[1] Current address: Technical Center, The BOC Group, 100 Mountain Avenue, Murray Hill, New Jersey 07974.

0021-9517/85 $3.00

calcination temperature upon the WO_3 on Al_2O_3 system (*3, 4*). At higher calcination temperatures (1050°C) and high loadings of tungsten oxide (i.e., 18% WO_3 on Al_2O_3), a solid state reaction to form $Al_2(WO_4)_3$ takes place (*3, 4*).

In the present investigation, the effect of calcination temperature upon the WO_3 on Al_2O_3 system was examined in greater detail with LRS, XPS, and XRD. Of particular interest were calcination temperatures of 900–1050°C where the γ-alumina support undergoes phase transitions and experiences dramatic decreases in surface area. The effect of these changes upon the nature of the surface tungsten oxide complex and the solid state chemistry of the WO_3 on Al_2O_3 system is examined in this paper.

II. EXPERIMENTAL

The tungsten oxide on γ-Al_2O_3 (Engelhard, reforming grade, ~180 m^2/g) catalysts were prepared by the incipient wetness impregnation method by adding an aqueous solution of ammonium meta-tungstate to the alumina powder. The catalysts were subsequently dried at 110°C and calcined in air at 500°C for 16 hr. The catalysts were further calcined between 650 and 1050°C for 16 hr to examine the influence of loss in surface area of the γ-alumina support upon the WO_3 on Al_2O_3 system.

XPS measurements were made with a Leybold-Heraeus LHS-10 electron spectrometer. The X-ray source was obtained from an aluminum anode operated at 12 kV and 25 mA, and the intensities and binding energies of the W $4f_{5/2,7/2}$ signals were reference to the Al $2p$ peak at 74.5 eV.

X-Ray powder diffraction patterns were obtained with a Philips diffractometer using Cu$K\alpha$ radiation and a diffracted beam monochromator.

Figure 1 shows the schematic diagram of the experimental setup of the multichannel laser Raman spectrometer. An argon ion laser (Spectra Physics, Model 165) was tuned to the 514.5-nm line for excitation. A prism monochromator (Anaspec Model 300S) which has a typical band width of 0.3 nm was used to remove the laser plasma lines. A cylindrical lens (f = 250 mm) and a variable spherical lens (f = 90–100 mm) were used to achieve an elliptically focused image on the sample. Each sample of about 0.2 g was pelletized under 10 kpsi pressure into a 13-mm-diameter wafer for mounting on a sample holder capable of spinning. Measurements were made in the stationary and spinning modes. The laser power at the sample location was set in the range 1–40 mW.

The scattered light was collected by a lens (F/1.2, f/55 mm) held at about 45° with respect to the excitation. The Raman spectrometer was a triple monochromator (Instruments SA, Model DL203) equipped with holographic gratings and F4 optics. The spectrometer was coupled to an optical multichannel analyzer (Princeton Applied Research, Model OMA2) equipped with an intensified photodiode array detector

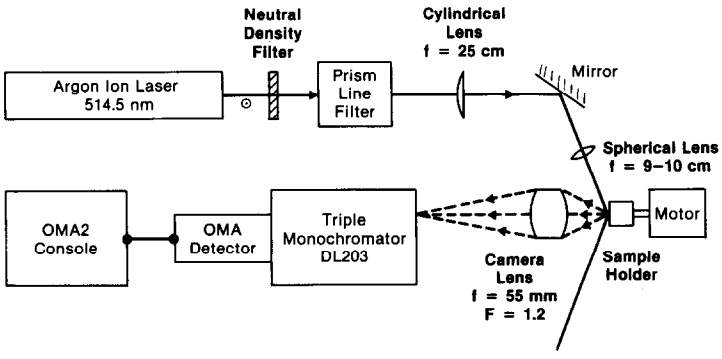

FIG. 1. Schematic of multichannel laser Raman spectrometer.

cooled to −15°C. This optical multichannel analyzer system could deliver a spectrum about a factor of 100 faster than the conventional scanning spectrometer and averaging capability permitted measurements on samples of weak signals. The total accumulation time needed for each spectrum reported here typically was about 100 sec or less. The digital display of the spectrum was calibrated to give 1.7 cm^{-1}/channel whereas the overall spectral resolution was about 6 cm^{-1}.

III. RESULTS

The surface area of alumina-supported tungsten oxide decreases dramatically at high calcination temperatures because of the collapse of the alumina structure as shown in Table 1 for 10% WO_3 on Al_2O_3 (2.6×10^{20} W atoms/g catalyst). XRD of the samples does not exhibit any tungsten oxide phases below a 1000°C calcination temperature. XRD of physical mixtures of bulk WO_3 and Al_2O_3 (as well as bulk $Al_2(WO_4)_3$ and Al_2O_3) showed that 1 wt% of the bulk tungsten oxide phases is detectable. The absence of bulk tungsten oxide phases implies that the supported tungsten oxide primarily exists in an amorphous, noncrystalline state or as small crystallites of less than 4 nm diameter for samples calcined below 1000°C. At calcination temperatures of 1000 and 1050°C crystalline $Al_2(WO)_4)_3$ is observed in the XRD patterns. The γ-alumina support simultaneously transforms to θ-Al_2O_3 at temperatures above 900°C. The X-ray photoelectron spectra of the supported tungsten oxide is presented in Fig. 2 for the samples calcined at 500 and 950°C. The features of the W $4f_{5/2,7/2}$ XPS spectra are identical for the two samples, but their intensities, relative to the alumina support, are different. The larger intensity of the sample calcined at 950°C reveals that the *surface density* of the surface tungsten oxide species on alumina increases with higher calcination temperatures (*9*). The binding energies of both XPS W $4f_{5/2,7/2}$ spectra occur at ~36.0 eV. This binding energy is consistent with that expected for W^{6+} in an alumina environment, but it cannot be used to distinguish between different W–Al–O structures (*5*).

TABLE 1

10% WO_3/Al_2O_3 Altered by High Calcination Temperature

Calcination temperature (16 hr) (°C)	BET (m^2/g)	XRD
500	170	γ-Al_2O_3
650	172	γ-Al_2O_3
800	130	γ-Al_2O_3
950	66	θ-Al_2O_3
1000	42	θ-Al_2O_3 + $Al_2(WO_4)_3$
1050	15	θ-Al_2O_3 + $Al_2(WO_4)_3$

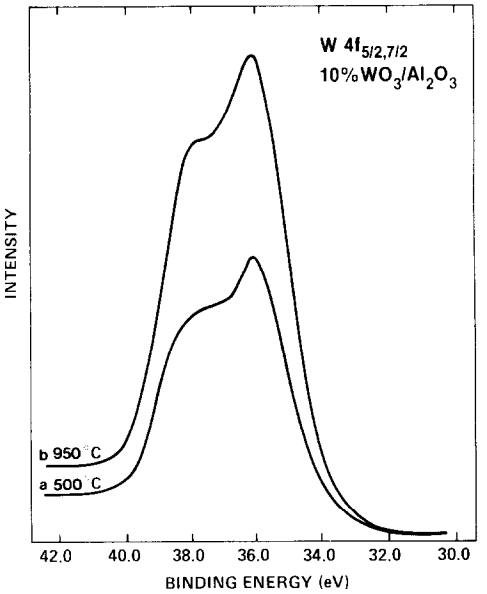

FIG. 2. Smoothed XPS W $4f_{5/2,7/2}$ spectra for 10% WO_3/Al_2O_3 calcined at (a) 500°C and (b) 950°C relative to alumina support.

Laser Raman spectroscopy, however, is very sensitive to the coordination of the tungsten oxide complex because it measures the vibrational modes of the tungsten–oxygen bonds. The laser Raman spectra for the 10% WO_3 on Al_2O_3 samples calcined at 650–1050°C are presented in Fig. 3. Note the very different laser Raman spectra for the WO_3 on Al_2O_3 system as the

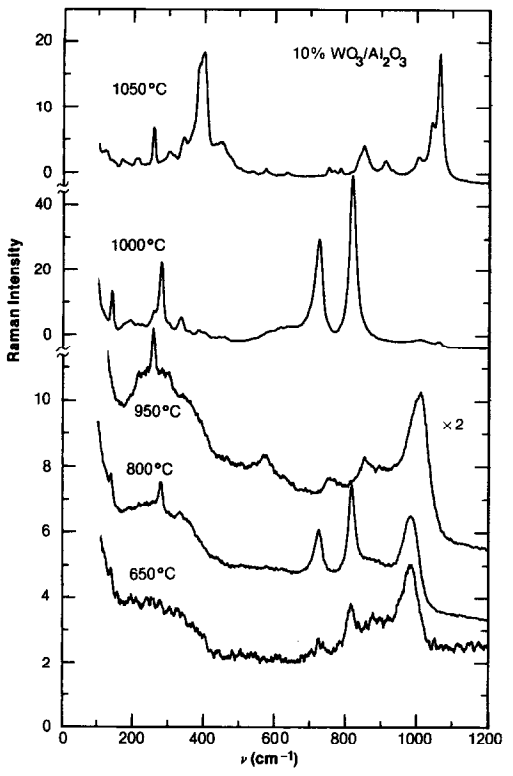

FIG. 3. Laser Raman spectra for 10% WO_3/Al_2O_3 as a function of calcination temperature.

calcination temperature increases. Before the spectra in Fig. 3 can be discussed, one must be familiar with the spectra for known tungsten oxide compounds.

The Raman spectra of the bulk oxides WO_3, $Al_2(WO_4)_3$, and Na_2WO_4 are presented in Fig. 4. The WO_3 structure (distorted ReO_3 structure) is made up of distorted corner shared WO_6 octahedra (*10*). The abundance of peaks in the Raman spectrum is a consequence of the appreciable distortion of the WO_3 structure from the ideal octahedral arrangement of ReO_3. The major vibrational modes of WO_3 are located at 808, 714, and 276 cm^{-1}, and have been assigned to the W–O stretching mode, the W–O bending mode, and the W–O–W deformation mode, respectively (*5*). Other minor bands are at 608, 327, 243, 218, 185, and 136 cm^{-1}. The $Al_2(WO_4)_3$ is a defect scheelite structure (distorted $CaWO_4$ structure) composed of distorted, isolated tetrahedral tungstate. The major Raman peaks of $Al_2(WO_4)_3$ can be assigned by comparison with tetrahedrally coordinated tungsten oxide in WO_4^{2-} (aq.) (*5*) and Na_2WO_4. WO_4^{2-} (aq.) and Na_2WO_4 exhibit major vibrational modes at 933 and 928 cm^{-1} (symmetric W–O stretch), 830 and 813 cm^{-1} (antisymmetric W–O stretch), 324 and 312 cm^{-1} (W–O bending vibrations), respectively. The additional Na_2WO_4 peak at 93 cm^{-1} is due to lattice vibrations of the solid. Thus, the $Al_2(WO_4)_3$ peak at 1055 cm^{-1} is attributed to the W–O stretching mode and the doublet at 378–394 cm^{-1} is assigned to the W–O bending modes.

The laser Raman spectra of γ-Al_2O_3 calcined at 500°C does not exhibit any Raman peaks (see Fig. 5), but calcination temperatures above 900°C produce a single sharp peak at 252 cm^{-1}. The Raman peak at 252 cm^{-1} is assigned to the θ-Al_2O_3 transitional phase. The broad background in the Raman spectra of alumina (400–1000 cm^{-1}) is due to fluorescence from the samples.

With the above information about the alumina support and tungsten oxide reference compounds, the laser Raman spectra for 10% WO_3 on Al_2O_3 in Fig. 3 can be discussed. The WO_3 on Al_2O_3 sample calcined

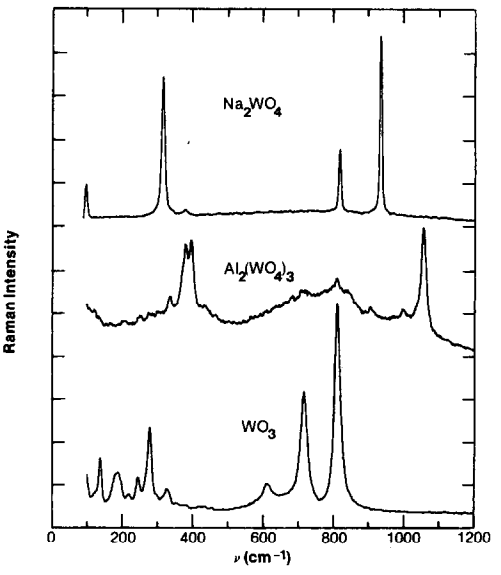

FIG. 4. Laser Raman spectra of standard compounds.

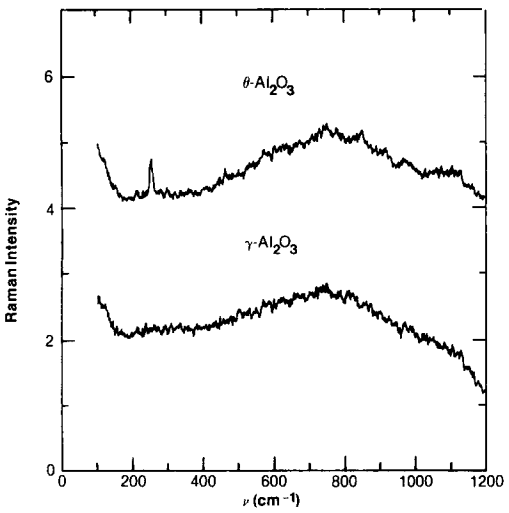

FIG. 5. Laser Raman spectra of γ-alumina and θ-alumina.

at 650°C exhibits Raman peaks at 972, 809, and 718 cm^{-1}. The peak at 972 cm^{-1} is associated with the tungsten oxide surface complex. The position of this Raman peak increases monotonically from 972 to about 1000 cm^{-1} as the calcination temperature is increased to 950°C. Similar shifts are observed when the tungsten oxide loading is increased for samples calcined at 500°C (*1–4*). These shifts are related to a decrease in hydration of the surface tungsten oxide species with increasing surface coverage, and the shift reaches a limit at approximately monolayer coverage (*7, 8*). At calcination temperatures of 1000 and 1050°C the Raman spectra are dominated by the bulk tungsten oxide phases WO_3 and $Al_2(WO_4)_3$. The Raman peaks at 811, 717, 273, and 137 cm^{-1} are characteristic of crystalline WO_3. These peaks decrease in intensity as the calcination temperature is increased to 950°C, and increase again at 1000°C. Note that at 950°C the crystalline WO_3 Raman peaks at 811, 717 and 273 cm^{-1} are absent, and instead small peaks at 846, 751, and 551 cm^{-1} are present. At the calcination temperature of 1050°C the crystalline WO_3 phase is again absent from the Raman spectra. The relatively strong signals of the WO_3 Raman peaks can be misleading because crystalline WO_3 possesses a Raman scattering cross-section that is much greater than $Al_2(WO_4)_3$, by ~32×, and the tungsten oxide surface species on alumina, by ~160× (*11*). In order to estimate the actual relative proportions of each phase in a mixed structure situation, the corresponding signals must be normalized by these factors. For the samples calcined at 650 and 800°C, the intensity of the crystalline WO_3 Raman signal varied from point to point, indicating the heterogeneity of these samples with respect to local crystalline WO_3 content. The crystalline WO_3 phase could not have been produced by localized heating of the sample by the laser because the crystalline WO_3 phase was absent from the 10% WO_3 on Al_2O_3 calcined at 950°C. The $Al_2(WO_4)_3$ phase, major Raman peak at 1055 cm^{-1}, is first observed at a calcination temperature of 1000°C and dominates the Raman spectra after a calcination temperature of 1050°C. The θ-Al_2O_3 Raman peak at 253 cm^{-1} is present in the spectra for calcination temperatures of 950–1050°C in agreement with the XRD data in Table 1. This series of Raman spectra reveals the dynamic nature of the WO_3 on Al_2O_3 system and its dependence upon the temperature of calcination.

The influence of tungsten oxide loading (4, 6, 10, and 15%) upon the Raman spectra of WO_3 on Al_2O_3 at several different calcination temperatures (800, 950, 1000, and 1050°C) are presented in Figs. 6–9. Comparison of Figs. 6–9 reveal that essentially the same Raman spectra can be obtained by varying either the calcination temperature or tungsten oxide loading. For example, (a) very similar Raman spectra are obtained by varying the calcination temperature for 10% WO_3 on Al_2O_3 or by varying the tungsten loading (4–15% WO_3) at a constant calcination temperature of 1000°C, and (b) the crystalline WO_3 phase dominates the Raman spectra of 6% WO_3 on Al_2O_3 calcined at 1050°C, 10% WO_3 on Al_2O_3 calcined at 1000°C, and 15% WO_3 on Al_2O_3 calcined at 950°C. These data reveal that the form of the alumina support is not crucial since the same Raman spectrum is observed for high

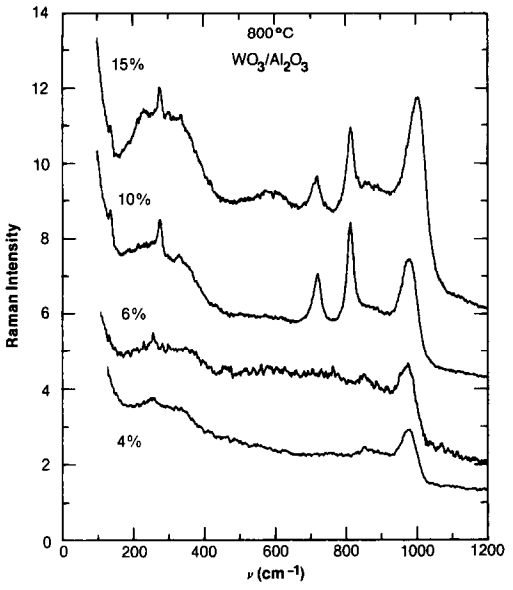

FIG. 6. Laser Raman spectra of WO_3/Al_2O_3 calcined at 800°C.

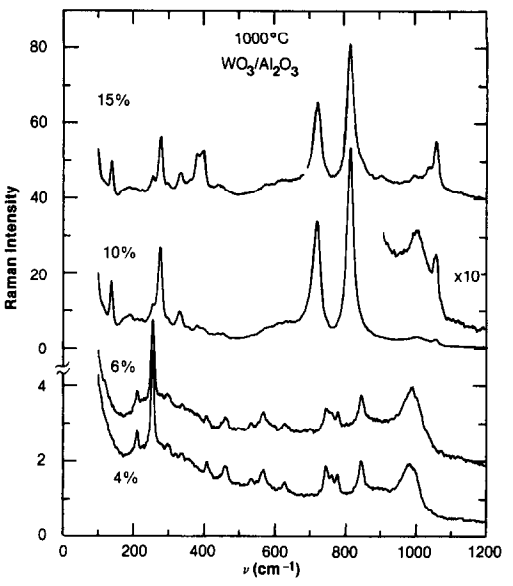

FIG. 8. Laser Raman spectra of WO_3/Al_2O_3 calcined at 1000°C.

tungsten oxide loading on γ-Al_2O_3 and low tungsten oxide loading on θ-Al_2O_3.

Furthermore, the quantity of the tungsten oxide surface complex present in the WO_3 on Al_2O_3 samples, at the different tungsten oxide loadings and calcination temperatures, is also displayed by the se-

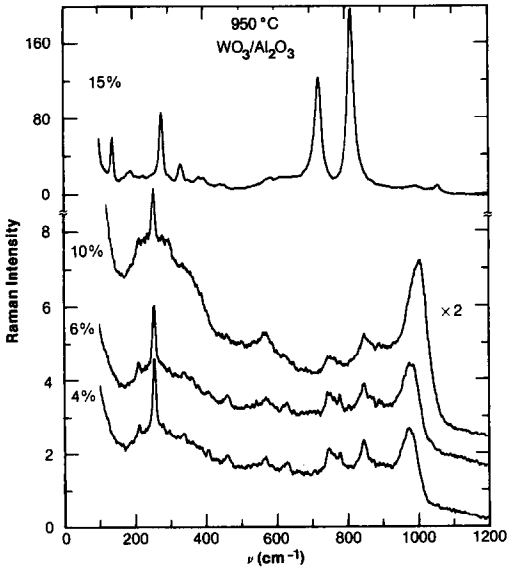

FIG. 7. Laser Raman spectra of WO_3/Al_2O_3 calcined at 950°C.

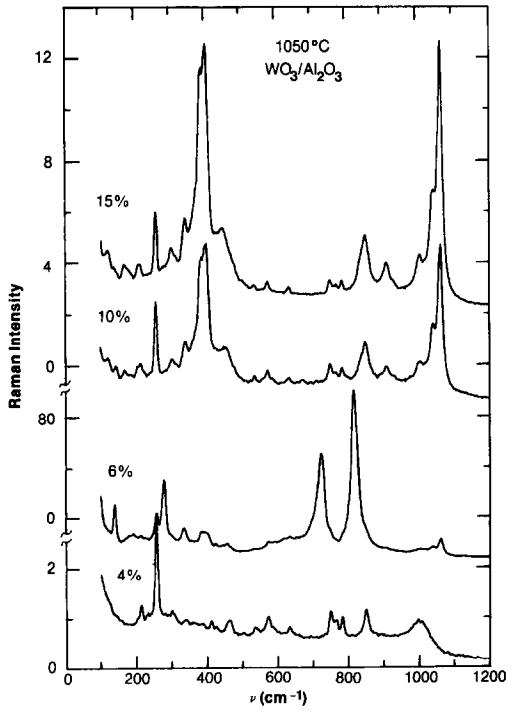

FIG. 9. Laser Raman spectra of WO_3/Al_2O_3 calcined at 1050°C.

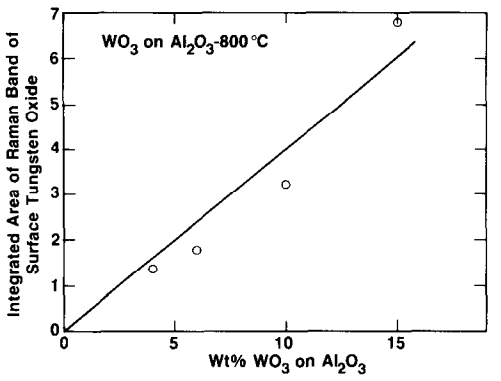

FIG. 10. Integrated Raman peak area (934–1026 cm^{-1}) for 4, 6, 10, and 15 wt% WO_3 on γ-Al_2O_3 calcined at 800°C.

ries of Raman spectra. Figure 10 shows the integrated areas for the surface phase tungsten oxide Raman band for the 4, 6, 10, and 15 wt% WO_3 on Al_2O_3 samples calcined at 800°C. Figure 11 shows the integrated areas for the surface phase tungsten oxide Raman band for the 4, 6, and 10 wt% WO_3 on Al_2O_3 samples calcined at 950°C, and for the 4 and 6 wt% WO_3 on Al_2O_3 samples calcined at 1000°C. The integrated Raman peak areas for the surface tungsten oxide phase are linear with tungsten oxide content for all three calcination temperatures, and suggest that the surface tungsten oxide complex on alumina is the major tungsten oxide phase for these WO_3 on Al_2O_3 samples.

IV. DISCUSSION

A model for the WO_3 on Al_2O_3 system is now developed from the laser Raman spectroscopy, X-ray photoelectron spectroscopy, and X-ray diffraction data. Below monolayer coverages of tungsten oxide on alumina (less than ~25–30% WO_3 on Al_2O_3) tungsten oxide is in a highly dispersed and amorphous state on the alumina surface for low calcination temperatures (500–800°C) (*5, 9*). This surface tungsten oxide complex is represented by a major Raman peak at ~965–1000 cm^{-1}. In addition, Raman peaks for crystalline WO_3 are also observed in this temperature range for the 10% and 15% WO_3 on Al_2O_3 samples. The bulk WO_3 Raman signal (major peaks at 811, 717, and 273 cm^{-1}) is due to small tungsten oxide crystallites that are still present on the catalyst surface after calcination which are not detected by XRD. These small WO_3 crystallites are observable because of the very high Raman scattering cross section of crystalline WO_3 (*11*). The amount of tungsten oxide present as crystalline WO_3 is estimated to be less than 1% of the total tungsten oxide content present in the 10 and 15% WO_3 on Al_2O_3 samples. As the calcination temperature increases, the relative amount of crystalline WO_3 initially decreases. Thus, at the higher calcination temperatures the WO_3 particles disperse on the alumina surface because of the affinity of tungsten oxide for alumina and the mobility of tungsten oxide at elevated temperatures. Simultaneously, there is a substantial decrease in the surface area of the alumina support. Interestingly, the strong interaction between tungsten oxide and alumina results in an increased dispersion of tungsten oxide on alumina at temperatures where there is a significant decrease in the surface area of the alumina support. The decrease in the surface area decreases the distance between the tungsten oxide surface species and increases the tungsten oxide surface density on the alumina support. This is reflected in the increase in the inten-

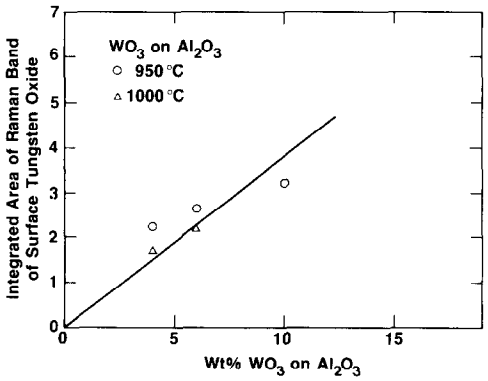

FIG. 11. Integrated Raman peak area (934–1026 cm^{-1}) for 4, 6, and 10 wt% WO_3 on Al_2O_3 calcined at 950°C (○), and for 4 and 6 wt% WO_3 on Al_2O_3 calcined at 1000°C (△).

TABLE 2

Raman Band of the Tungsten Oxide Surface Complex Shifts with Tungsten Oxide Surface Density

Temperature (°C)	4% WO_3/Al_2O_3	6% WO_3/Al_2O_3	10% WO_3/Al_2O_3	15% WO_3/Al_2O_3
650	970	967	972	—
800	975	971	975	1000
925	—	972	988	—
950	972	974	1002	991
975	—	975	1000	—
1000	983	986	999	996
1050	999	1000	—	—

sity of the XPS W $4f_{5/2,7/2}$ signal relative to the alumina support (see Fig. 2), and the shift from ~965 to ~1000 cm^{-1} in the Raman band associated with the tungsten oxide surface complex (see Table 2 and Figs. 3, 6–9). These structural changes in the WO_3 on Al_2O_3 system are depicted in Figs. 12a and b.

A close-packed monolayer of tungsten oxide on alumina is formed when the minimum possible distance between tungsten centers is achieved. The lower the tungsten oxide loading, the more severe the calcination temperature must be to reach the close-packed monolayer for a given support. At monolayer coverage the Raman band for the surface tungsten oxide shifts to ~1000 cm^{-1} (*1–3*). This suggests that to achieve a close-packed monolayer, the 4% WO_3 on Al_2O_3 must be heated to ~1050°C, 6% WO_3 on Al_2O_3 must be heated to between 1000 and 1050°C, 10% WO_3 on Al_2O_3 must be heated to ~950°C, and 15% WO_3 on Al_2O_3 must be heated to ~800°C (see Table 2). From the surface areas of 15% WO_3 on Al_2O_3 sample calcined at 800°C (128 m^2/g), the 10% WO_3 on Al_2O_3 sample calcined at 950°C (66 m^2/g), and the 4% WO_3 on Al_2O_3 sample calcined at 1050°C (31 m^2/g), the surface density of tungsten is calculated to be $(4.0 \pm 0.4) \times 10^{18}$ W atoms/m^2 at monolayer coverage of tungsten oxide on alumina. This value is in agreement with the monolayer value determined by Salvati *et al.* from a plot of XPS (W 4*f*)/(Al 2*p*) intensity ratios (4.3×10^{18} W atoms/m^2) (*5*). The surface density of oxygen anions on the (111) plan of Al_2O_3 is 18×10^{18} sites/m^2. Thus, one tungsten oxide surface complex occupies approximately 4–5 sites on the alumina surface when a close-packed monolayer is formed. In practice, it is difficult to stop the alumina desurfacing process to yield exclusively the close-packed tungsten oxide monolayer at these high temperatures.

The formation of the close-packed tungsten oxide monolayer does not preclude the alumina from additional loss in surface area

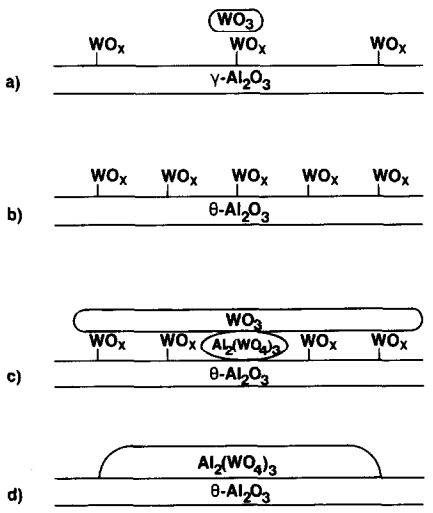

FIG. 12. Structural transformation of tungsten oxide on alumina as a function of calcination temperature. For 10% WO_3/Al_2O_3: (a) 500–800°C, (b) 950°C, (c) 1000°C, and (d) 1050°C.

at still higher temperatures. The close-packed tungsten oxide monolayer accommodates the further desurfacing by forming the bulk tungsten oxide phases WO_3 and $Al_2(WO_4)_3$ as depicted in Figs. 12c and d. The WO_3 crystallites are readily detected by laser Raman spectroscopy (see Figs. 6–9), but not by XRD (see Table 1) (*3, 4*). For the 10% WO_3 on Al_2O_3 sample, it is estimated that LRS can detect less than 0.1% crystalline WO_3, but XRD can detect ~1% crystalline WO_3 (crystallites ≥4 nm). The $Al_2(WO_4)_3$ phase can be detected with about equal sensitivity by laser Raman spectroscopy and XRD (0.3–1.0% $Al_2(WO_4)_3$ for 10% WO_3 on Al_2O_3).

The conclusion that the tungsten oxide surface complex is the major tungsten oxide phase for WO_3 on Al_2O_3 samples of ≤10 wt% WO_3 content when calcined up to 1000°C is supported by the observation that the integrated Raman peak areas for the surface tungsten oxide phase are linear with tungsten oxide content for samples calcined at 800, 950, and 1000°C (see Figs. 10 and 11). If a significant amount of tungsten oxide on the alumina support was not present as the surface tungsten oxide complex then deviations from linearity in the integrated Raman peak areas with either tungsten oxide content or calcination temperature would be expected. The same conclusion was reached in previous work when the integrated Raman band of the surface phase tungsten oxide on Al_2O_3 was identical for a 25% WO_3 on Al_2O_3 sample desurfaced beyond the monolayer limit where crystalline WO_3 was found and a 15% WO_3 on Al_2O_3 sample desurfaced to the same surface area to the monolayer coverage limit (i.e., no crystalline WO_3 formed) (*11*). This earlier observation also supports the present conclusion that the surface phase tungsten oxide on Al_2O_3 transforms to crystalline WO_3 only when the monolayer coverage limit is exceeded.

Additional insight into the solid state reactions responsible for the formation of $Al_2(WO_4)_3$ is provided by controlled atmosphere electron microscopy (CAEM) studies (*12*). The *in situ* CAEM studies revealed that at high temperature the WO_3 particles react with the Al_2O_3 support by migration of alumina into the WO_3 particles. Thus WO_3 crystallites must be present in the WO_3 on Al_2O_3 sample for $Al_2(WO_4)_3$ formation to occur. Further heating of the WO_3 on Al_2O_3 samples results in the conversion of all the tungsten oxide phases to $Al_2(WO_4)_3$, the only stable tungsten oxide compound for the W–Al–O system. Thus, the model presented in Fig. 12 shows the evolution of the WO_3 on Al_2O_3 system with calcination temperature and tungsten oxide loadings. The important parameter controlling the phases present in the WO_3 on Al_2O_3 system is the *surface density* of the tungsten oxide species on the alumina surface.

Iannibello *et al.* also examined the influence of high calcination temperature (1050°C) upon the phases present in the WO_3 on Al_2O_3 system with laser Raman spectroscopy (*4*). They found that the tungsten oxide complex on the alumina surface was stable to high calcination temperatures for samples containing 7% WO_3 on Al_2O_3. However, for samples containing 18% WO_3 on Al_2O_3 the tungsten oxide surface complex was converted to $Al_2(WO_4)_3$ at these high temperatures. The present laser Raman results agree very well with that reported by Iannibello *et al.* [The differences that exist between the two studies are probably due to the use of different sources of γ-aluminas and different preparation procedures in the two studies.] In addition, the present, more detailed, study reveals that the tungsten oxide surface complex is not directly converted to $Al_2(WO_4)_3$ as was proposed by Iannibello *et al.* (*4*). Prior to the formation of $Al_2(WO_4)_3$, the surface tungsten oxide complex forms a close-packed monolayer with WO_3 crystallites only forming when the monolayer coverage limit is exceeded. The presence of the WO_3 crystallites are apparently required before $Al_2(WO_4)_3$ is formed as observed directly by CAEM. Thus, the 7% WO_3 on Al_2O_3 sample

studied by Iannibello *et al.* (*4*) did not form $Al_2(WO_4)_3$ after a 1050°C calcination because the alumina support did not desurface sufficiently to form crystalline WO_3 particles. The model developed for the WO_3 on Al_2O_3 system in the present study extends our understanding of this complex oxide–oxide interaction, and may find applicability in describing other similar oxide–oxide systems.

The Raman spectra of several WO_3 on Al_2O_3 samples also exhibit a series of weak bands between 400 and 850 cm^{-1} (i.e., 4, 6, and 10% WO_3 on Al_2O_3 calcined at 950°C, 4 and 6% WO_3 on Al_2O_3 calcined at 1000°C, and 4% WO_3 on Al_2O_3 calcined at 1050°C). The origin of this series of weak Raman bands is not completely understood at present, but are suspected to represent very small, and, therefore, distorted WO_3 crystallites. For such distorted WO_3 crystallites, the degeneracy of the Raman active modes could be removed, and these bands could then be split into substates with shifted vibrational frequencies. Furthermore, some modes originally Raman inactive can become Raman active for such distorted crystallites. The presence of such small, distorted WO_3 crystallites in WO_3 on Al_2O_3 samples does not alter the model developed for the WO_3 on Al_2O_3 system.

V. CONCLUSIONS

The influence of calcination temperature upon the solid state chemistry of WO_3 on Al_2O_3 was elucidated with laser Raman spectroscopy. Laser Raman spectroscopy revealed the amorphous and crystalline structural transformations occurring in the WO_3 on Al_2O_3 oxide system. Below monolayer coverage of tungsten oxide on alumina, the tungsten oxide phase is present as a highly dispersed and amorphous surface complex on the support. A close-packed monolayer of the tungsten oxide surface complex on alumina is formed as the surface area of the alumina support decreases at high calcination temperatures. The lower the tungsten oxide loading, the more severe the calcination temperature must be to reach the close-packed monolayer. The close-packed tungsten oxide monolayer accommodates the further desurfacing at still higher temperatures by forming the bulk tungsten oxide phases WO_3 and $Al_2(WO_4)_3$. The $Al_2(WO_4)_3$ phase is formed from the reaction of WO_3 crystallites with the Al_2O_3 support. The parameter controlling the phases present in the WO_3 on Al_2O_3 system is the *surface density* of the tungsten oxide species on the alumina surface.

REFERENCES

1. Thomas, R., Kerkhof, J. M., Moulijn, J. A., Medema, T., and DeBeer, V. H. J., *J. Catal.* **61,** 559 (1980).
2. Thomas, R., DeBeer, V. H. J., and Moulijn, J. A., *Bull. Soc. Chim. Belg.* **90,** 1349 (1981).
3. Iannibello, A., Villa, P. L., and Marengo, S., *Gazz. Chim. Ital.* **109,** 5121 (1979).
4. Tittarelli, P., Iannibello, A., and Villa, P. L., *J. Solid State Chem.* **37,** 95 (1981).
5. Salvati, L., Makovsky, L. E., Stencil, J. M., Brown, F. R., and Hercules, D. M., *J. Phys. Chem.* **85,** 3700 (1981).
6. Biloen, P., and Pott, G. T., *J. Catal.* **30,** 169 (1973).
7. Wang, L., and Hall, W. K., *J. Catal.* **82,** 177 (1983).
8. Chan, S. S., Wachs, I. E., Murrell, L. L., Wang, L., and Hall, W. K., *J. Phys. Chem.* **88,** 5831 (1984).
9. Murrell, L. L., Grenoble, D. C., Baker, R. T. K., Prestridge, E. B., Fung, S. C., Chianelli, R. R., and Cramer, S. P., *J. Catal.* **79,** 203 (1983).
10. Schiavello, M., *Chim. Indust.* **61,** 554 (1979).
11. Chan, S. S., Wachs, I. E., and Murrell, L. L., *J. Catal.* **90,** 150 (1984).
12. Soled, S., Murrell, L. L., Wachs, I. E., McVicker, G. B., Sherman, L. G., Chan, S. S., Dispenziere, N. C., Jr., and Baker, R. T. K., *ACS Symp. Ser.*, in press.